

Solitonlike pulses in perturbed and driven Hertzian chains and their possible applications in detecting buried impurities

Surajit Sen,^{1,2,*} Marian Manciu,¹ and James D. Wright^{1,3}

¹*Department of Physics, State University of New York at Buffalo, Buffalo, New York 14260*

²*Center for Advanced Photonic and Electronic Materials, State University of New York at Buffalo, Buffalo, New York 14260*

³*B1-8 Keynes College, University of Kent, Canterbury, Kent CT2 7NZ, United Kingdom*

(Received 17 July 1997)

We present detailed numerical studies on the motion of an initial perturbation in a chain of spheres which are characterized by Hertzian contacts. We consider the propagation of the perturbation in the presence and in the absence of gravitational compaction in the chain [see R. S. Sinkovits and S. Sen, *Phys. Rev. Lett.* **74**, 2686 (1995)]. Our results show that robust solitonlike pulses carry the initial perturbation from the surface to the depths of the Hertzian chains for various magnitudes of the initial perturbation at finite loadings of the column. In addition, we probe the structural characteristics of the solitonlike pulse as a function of the magnitude of the initial impact, of loading, and of the gravitational field. Our results suggest that the solitonlike features, while altered, persist at finite gravitational fields when the compaction of grains with increasing depth becomes important. In the presence of light mass impurities in the Hertzian chain, we present evidence of backscattering of the solitonlike pulse and suggest that acoustic backscattering can be a possible probe of buried light mass impurities in granular beds. In closing, we discuss the propagation of perturbations in finite Hertzian chains when the surface grain is coupled to a transducer which vibrates with very low amplitude and frequency, and we report the formation of metastable standing-wave-like patterns in finite Hertzian chains.

[S1063-651X(98)12202-X]

PACS number(s): 46.10.+z, 03.40.Kf, 43.25.+y

I. INTRODUCTION

Nonlinear elasticity and sound propagation in dry granular columns at small loadings [1–8] has emerged as a subject of increasing attention in recent years. It has been noted by Nesterenko [2] that the propagation of a perturbation in a loaded chain of Hertzian contacts possesses solitonlike features. The studies of Miller [9], Sinkovits and Sen [5], and Coste *et al.* [8] have independently confirmed the presence of these solitonlike pulses. In particular, Sen and Sinkovits [6] have carried out particle-dynamics-based studies which show that these solitonlike pulses are present in gravitationally compacted granular columns.

As of now, there are a handful of physical systems which are known to support solitonic pulses [10]. The presence of solitonlike pulses in perturbed Hertzian systems therefore presents interesting possibilities [2,5,6,8,9,11]. One such possibility is to use the solitonlike pulses, which can travel through the granular contacts with minimal dispersion, to probe buried objects that may be undetectable using the more frequently used electromagnetic probes. Metal-poor landmines in dry granular beds are examples of underground objects which may become detectable using acoustic backscattering of solitonlike pulses.

To explore the prospects for the application of solitonlike pulses for detecting certain buried objects in granular beds, it is imperative that one must acquire a detailed understanding of the following three aspects. First, the conditions under

which these solitonlike pulses can be initiated and sustained. Second, to determine whether the solitonlike pulses are partially reflected or backscattered by impurities. Third, transducers are commonly used devices for exciting the surface-based grains and thus it is very important to address the issue of what kind of amplitudes and frequencies are appropriate for such transducers for minimizing the attenuation of the solitonlike pulses. The present study is a first step toward the exploration of these fascinating issues.

In this paper, we present particle-dynamics-based studies on the propagation of perturbations in chains of linearly aligned spherical beads (we shall refer to these systems as granular chains in the rest of this paper). The intergrain interactions in our model are characterized via the Hertzian contact law [12], and have been used to successfully model assemblies of glass and stainless steel spheres as well as sand grains. The definition of these contacts is given in Sec. II below. We address the effects of constant loading across a granular chain at zero gravitational field and study the effects of finite gravitational fields on the properties of the solitonlike pulse. This work also presents simulational results on the backscattering of the solitonlike pulse from impurities in the granular chain. In closing, we present some preliminary results which suggest that low frequency, low amplitude pulses injected into gravitationally compacted finite granular chains lead to metastable standing-wave-like patterns. Our calculations suggest that “soliton pulse spectroscopy” possesses the potential for probing buried objects in granular beds.

The details of the models studied and the particle dynamics simulations are presented in Sec. II. The results of our study are presented in Secs. III–VI. Section III discusses the

*Author to whom correspondence should be addressed.

geometric properties of the pulse for various initial velocities of the first grain at different constant loadings and at zero gravitational fields. Section IV presents the time evolution of the pulse as it passes through light and heavy impurity masses at zero gravitational fields. Section V addresses the scattering of a solitonlike pulse in a vertical gravitationally compacted column with a few light mass impurities. Section VI discusses the propagation of perturbations generated by a transducer attached to the surface grain in a vertical gravitationally compacted column. Section VII closes with a summary of the work and the direction of ongoing and future research.

II. THE MODEL AND THE SIMULATIONS

A. Intergrain interactions

We model the granular chain as a collection of spheres which are either placed in contact with one another via some form of loading while the chain is oriented horizontally, or are oriented vertically and loaded by gravitational compaction. We follow the classic work of Hertz [12] and describe the energy associated with the repulsive interaction between any two compressed spheres labeled i and $i+1$ of radii R_i and R_{i+1} (while they are uncompressed) as follows. We define the ‘‘overlap’’ between the two adjacent grains by $\delta_{i,i+1}$, which can be written as $\delta_{i,i+1} \equiv R_i + R_{i+1} - r_{i,i+1}$, where we let $r_{i,i+1}$ represent the distance between the centers of the two spheres. The interaction energy between the granular spheres is expressed as a function of this overlap as follows:

$$V(\delta_{i,i+1}) = \frac{2}{5D} \left(\frac{R_i R_{i+1}}{R_i + R_{i+1}} \right)^{1/2} \delta_{i,i+1}^{5/2} \equiv a \delta_{i,i+1}^{5/2}, \quad (1)$$

where the constant $a \equiv (2/5D) \sqrt{R_i R_{i+1} / (R_i + R_{i+1})}$ and where

$$D = \frac{3}{4} \left(\frac{1 - \sigma_i^2}{E_i} + \frac{1 - \sigma_{i+1}^2}{E_{i+1}} \right), \quad (2)$$

in which σ_i , σ_{i+1} and E_i , E_{i+1} are Poisson’s ratios and Young’s moduli of the two bodies, respectively. The potential energy $V(\delta_{i,i+1}) = 0$ when $r_{i,i+1} > R_i + R_{i+1}$. The $V(\delta_{i,i+1}) \sim \delta_{i,i+1}^{5/2}$ law in Eq. (1) arises due to purely geometrical effects and is an exact result for perfectly spherical grains [for a detailed derivation of Eq. (1), see Ref. [12]]. As noted by Coste *et al.* [8], the interaction energy in Eq. (1) is expected to remain valid when the repulsive force and $\delta_{i,i+1}$ vary relatively slowly in time, in comparison with the time it takes for a bulk longitudinal acoustic wave to travel across a diameter of a spherical grain. We also neglect plastic deformation of the spheres in this study. The experimental work of Coste *et al.* [8] seems to suggest that this is a reasonable approximation for certain materials such as steel spheres. However, plastic deformation may play an important role in studying sound propagation in softer granular materials. These effects will be addressed in a separate publication [13].

B. Equations of motion and initial conditions

In this paper, we focus on the propagation of a perturbation that is initially impacted to the first grain of a granular chain. We present studies in which (i) the granular chain is uniformly loaded but gravitational compaction is absent, i.e., when the chains are horizontal, and in which (ii) gravitational compaction is present and provides the mechanism for progressively higher loading of the grains as the depth increases, i.e., the chains are vertical. In case (i), loading the grains in such a way that they are in intimate contact with one another is an important issue. The equation of motion of a grain of mass m at location z_i for case (i) is given by

$$m\ddot{z}_i = a[\{\Delta_0 - (z_i - z_{i-1})\}^{3/2} - \{\Delta_0 - (z_{i+1} - z_i)\}^{3/2}], \quad \text{case (i),} \quad (3)$$

$$m\ddot{z}_i = a[\{\Delta_0 - (z_i - z_{i-1})\}^{3/2} - \{\Delta_0 - (z_{i+1} - z_i)\}^{3/2}] - mg, \quad \text{case (ii).}$$

In Eq. (3), we define $\Delta_0 \equiv R_i + R_{i+1} - l_0$, where l_0 enters due to loading for the horizontal chain problem and we replace $R_i + R_{i+1}$ in the definition of $\delta_{i,i+1}$ given above Eq. (1) by Δ_0 . As we shall see, l_0 plays an important role in distinguishing between the shocklike perturbations and the softer compression pulses that can be generated down a column with suitable initial impact velocities on the first grain in the chain. For the vertical column problem in case (ii), in which gravitational compaction plays an important role, we add $-mg$ to the right-hand side of Eq. (3).

In case (i), given Δ_0 , the initial positions of all the grains in the chain are specified. The velocity of the first grain is specified at time $t=0$. The velocities of all the other grains are initially set to zero. For a given loading or l_0 , the velocity of the first grain therefore defines the physical properties of the solitonlike pulse. We discuss these properties in detail in Sec. III.

The initial structure of the vertically oriented granular chain [case (ii)] is quite different [5,6]. In this case, the grain at the bottom of the chain is most compressed while the one at the surface of the chain is least compressed. Since dry granular systems, being macroscopic, are largely insensitive to changes in temperature, it is extremely important to determine the ground state of a gravitationally compacted granular column. We accomplish this as follows. The location of the bottom grain is first fixed and the positions of the remaining grains are set such that the repulsive forces due to the overlap between the adjacent grains exactly equal the forces required to support the grain column. For a system of N grains in which the bottom grain is labeled 1, the overlap between grains i and $i+1$ is determined via the 1D sum rule as follows [5,6]:

$$g \sum_{j=i+1}^N m_j = \frac{5}{2} a \delta_{i,i+1}^{3/2}. \quad (4)$$

The reader may observe that if the gravitationally compacted chain is loaded, then it is essential to take into account the

additional repulsive force term that must arise from that loading [as described in case (ii) of Eq. (3)] on the left-hand side of Eq. (4) above. We do not consider loaded gravitationally compacted chains in this study.

The results presented in Sec. III [case (i)] and in Secs. IV and V [case (ii)] address the solutions to Eq. (3) in the absence of gravitational compaction and in the presence of gravitational compaction, respectively. In the zero gravitational compaction problem, Eq. (3) can be analyzed in the strongly nonlinear limit, if one assumes that the characteristic size of the perturbation is much greater than R_i . This analysis can be found in the work of Nesterenko [2] and in Ref. [8]. We refer the reader to these articles for the detailed analytical treatment and move on to further details of our numerical studies at this stage.

C. Program units

Our results are based upon careful numerical integration of the coupled equations of motion for granular chains with N spheres, where $N \sim 10^3$. We have used the third-order Gear predictor-corrector algorithm [14] for our dynamical studies. The data are represented in program units throughout this paper. We have set one program unit of distance as 10^{-5} m, one program unit of mass as 2.36×10^{-5} kg, and one program unit of time as 1.0102×10^{-3} s.

In our calculations, we set the grain diameter $2R_i = 100$ (expressed in program units), the gravitational acceleration $g = 1$ if it is included in the study (which corresponds to 9.8 m/s^2), and the mass m of each grain to 1 (which corresponds to 0.236×10^{-4} kg). In Eq. (1), we set the constant $a = 5657$. The integration time step has been kept at 1.25×10^{-5} in most of our calculations, unless specified otherwise. Choosing a smaller time step does not appear to improve or affect the accuracy of our calculations for the studies presented here. Choosing a time step that is a decade larger, however, results in poorer resolution of the features of the solitonlike pulses of interest.

III. SOLITONLIKE PROPAGATION AT CONSTANT LOADINGS

The advantage of a numerical study of propagation of solitonlike perturbations in a Hertzian chain over an analytical treatment lies in the fact that one can probe almost any aspect of the system dynamics. The findings presented in this section concern the details of the shapes of the solitonlike pulses at different loadings (described via Δ_0 or l_0) and at different magnitudes of the initial impact on the first grain in a horizontally oriented Hertzian chain, which is denoted by v_{imp} .

Our studies using chains with 1000 grains reveal that loading and the impact velocity of the first grain play crucial roles in determining the characteristics of the solitonlike pulse. These observations are in qualitative agreement with the findings of Miller [9]. We first focus on the results at very low loadings.

A. Solitonlike pulse at infinitesimal loadings: Shocklike regime

At very low loading, say $l_0 = 10^{-6}$ [see Eq. (3)], the grains are barely in contact with one another. If a large initial

velocity is given to the first grain, then our calculations indicate that the kinetic energy associated with the initial perturbation far exceeds the potential energy associated with the compression between the adjacent grains. As shown in Figs. 1(a)–1(c), in this “shock wave” regime, the shape of the collection of grains which are off-equilibrium looks very nearly like a temporally expanding rectangular object. In each of the cases probed, the rectangular pulse moves through the uniformly loaded chain at a fixed velocity c . The velocity associated with the propagation is dependent upon v_{imp} , where v_{imp} refers to the initial velocity of the first grain at time $t=0$. We study cases in which for $l_0 = 10^{-6}$, $v_{\text{imp}} = 10^{-3}$, 10^{-2} , and 10^{-1} are considered. For infinitesimal loadings, our calculations reveal that c is independent of l_0 and is strongly sensitive to v_{imp} . Larger magnitudes of v_{imp} caused larger sound propagation velocities in our studies. One would expect, however, that the magnitude of c would become insensitive to v_{imp} for hard-core spheres, i.e., when the potential diverges for all finite overlaps. Figure 1(d) shows the dependence of the pulse velocity $c \sim v_{\text{imp}}^\alpha$. We find that α is very close to 0.2 for the Hertzian chain systems that we have probed.

The width $W(t)$ of the expanding rectangular pulse (ignoring the tail-like structure at the end of each pulse) which represents the shock front is a measure of the diffusion coefficient of the perturbation in the Hertzian chain. The tail-like structure of the pulse is not a major concern in the infinitesimal loading regime because the velocity of the tail-like part is also a constant in time. As we shall see later, for larger loadings, the dynamics of the tail-like structure would be more complex. Our numerical studies reveal that

$$W(t) \sim t, \quad (5)$$

in the infinitesimal loading regime, i.e., for large v_{imp} cases. This is an expected result in view of the fact that the sound velocity remains fixed as the pulse propagates down the chain.

As l_0 is increased to 10^{-5} , the shapes of the propagating pulses as shown in Figs. 1(a)–1(c) are no longer preserved. The most noticeable change is seen at larger v_{imp} as shown near the beginning of the chain in Fig. 2(a). The “shock wave” part of the pulse is followed by regions of even higher overlap between some grains before a regime of progressively low overlaps emerges. These effects are also barely visible in Figs. 1(a)–1(c).

To understand these features we simply observe that the part of the granular chain that lies behind the pulse and has suffered a compression oscillates between the location of the unperturbed first grain (i.e., with respect to its location at $t < 0$) and the progressively increasing length of the perturbed region of the chain in the direction of the propagation. For smaller magnitudes of v_{imp} and fixed l_0 , the decreased ratio of v_{imp}/L_0 prevents the formation of the larger overlaps [see Figs. 2(b) and 2(c)] at intermediate length scales as in Fig. 2(a). We now turn our attention to the tails that develop at the rear end of the pulses in Figs. 2(b) and 2(c). The physical meaning of the tails in Figs. 2(b) and 2(c) becomes clear when we recognize that after the shock front has passed by a given point in the chain, the particles begin to return to their equilibrium positions. As we shall see, many of the

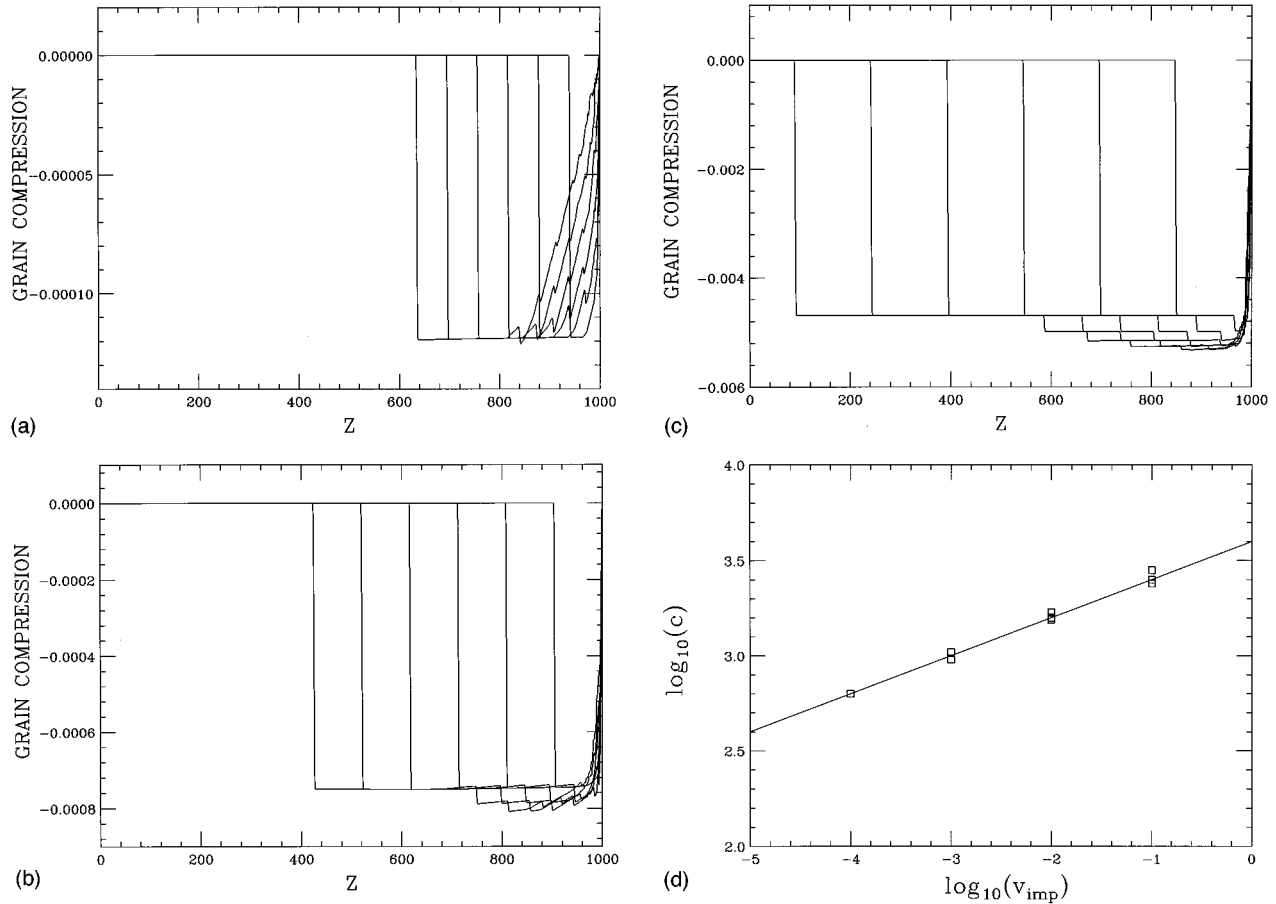


FIG. 1. Data showing the propagation of a broad rectangular pulse from right to left at various times in a Hertzian chain with $l_0 = 10^{-6}$ (in program units) [see Eq. (3)]. The x axis refers to the grain position, where the first grain is labeled as 1000 and the last one as 0. The y axis refers to the position of each grain (in program units) with respect to their original equilibrium location in the chains. In (a) $v_{\text{imp}} = 10^{-3}$, (b) $v_{\text{imp}} = 10^{-2}$, and in (c) $v_{\text{imp}} = 10^{-1}$. In (d) we show a plot of $\ln c$ versus $\ln v_{\text{imp}}$ for $l_0 = 10^{-6}$, 10^{-5} , and 10^{-4} . The data for various l_0 's have been lumped together because the differences in loading have no significant effect on c . The solid line yields a slope of 0.2.

more interesting aspects associated with the dynamics of the granular chain are buried in the information contained in these tails. To explore these tails in further detail we consider smaller loadings. These issues are discussed in Sec. III B.

B. Solitonlike pulse at larger and intermediate loadings: Compressive regime

For $l_0 = 10^{-4}$ and 10^{-3} and $v_{\text{imp}} = 10^{-3}$ and 10^{-2} , respectively, i.e., for $v_{\text{imp}}/l_0 \sim 10$, we find that the propagating pulses develop long tails. The results from these calculations are shown in Figs. 3(a) and 3(b). The grains that are located at the tail of the pulse suffer displacements in both directions with respect to their equilibrium positions at fixed loadings. The tails are especially prominent when l_0 is fairly large, being $O(10^{-3})$, and v_{imp} is only about an order of magnitude larger than l_0 [see Fig. 3(b)]. This is the regime in which the compression between the grains plays an important role and hence we shall refer to this parameter range as the *compressive regime*. Our studies suggest that the details of the tails are sensitive to the particulars of the granular masses and contacts. We therefore contend that the pulses with long tails are strong candidates for acoustic detection studies.

Analyses of the data in Figs. 3(a) and 3(b) reveal interesting results. We have made semilogarithmic plots of the magnitudes of grain displacements along the direction of compression (negative side of the y axis) with depth. The plots reveal that the tails at various depths and times are well fitted by exponential decays in depth. We refer to the *pulse function* as $P(z, t)$, z being the length of the chain, as

$$P(z, t) \sim \exp(-z/ct), \quad (6)$$

where c defines the velocity associated with the motion of the pulse along the chain. Time elapsed since the perturbation was effected is denoted by t .

Finally, we present data that describe the features of the propagating perturbation when $l_0 = 10^{-3}$ and $v_{\text{imp}} = 10^{-1}$, i.e., in a regime of v_{imp}/l_0 in which both the ‘‘shock-wave-like’’ features and the compression effects are clearly visible. This is shown in Fig. 4, in which we have used a longer chain of 3000 grains. The reflected pulse from a rigid boundary is presented in these data. The calculations suggest that the flat top of the in-going pulse is altered to a sloping top at reflection. This suggests that the shock-wave-like feature of the pulse is altered and the individual grains suffer differing overlaps at impact and illustrates the various subtle dynamical effects associated with the reflection of solitonlike pulses.

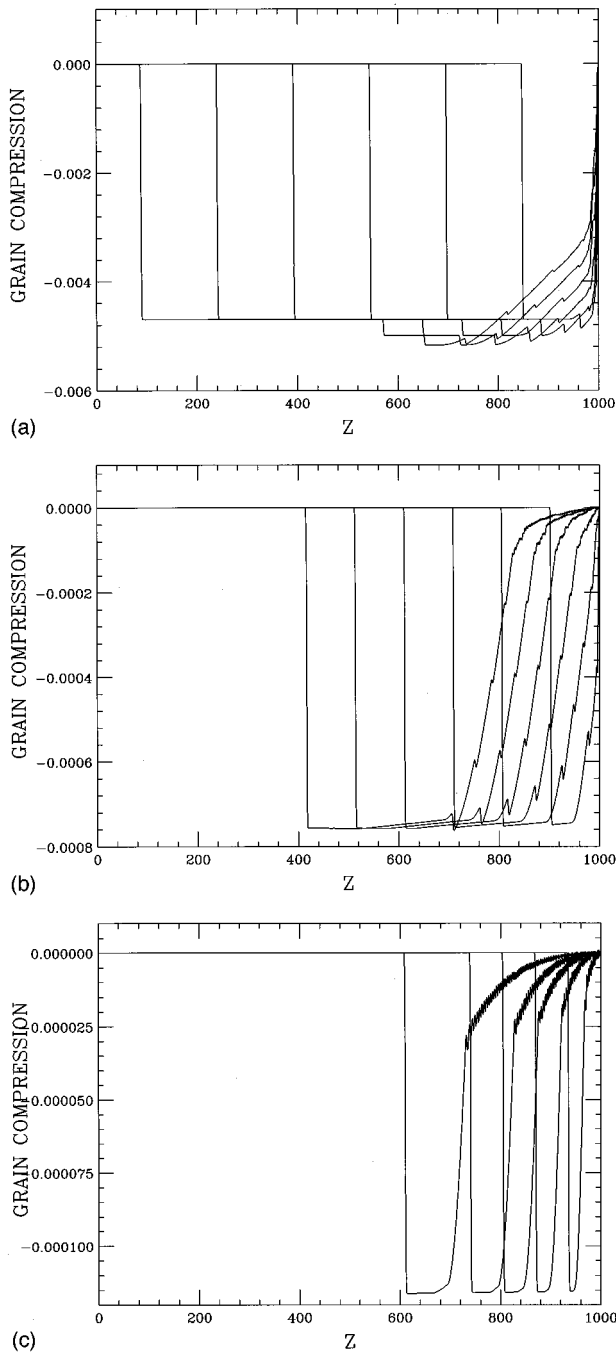


FIG. 2. Data showing the propagation of a pulse from right to left in a Hertzian chain with $l_0 = 10^{-5}$ (in program units) at various times. As in Figs. 1(a)–1(c), the x axis refers to the grain position and the y axis to the grain displacements (in program units) with respect to their original equilibrium positions. (a) shows additional compressions when $v_{\text{imp}} = 10^{-1}$, especially in the three leading pulses. These compressions arise due to additional weaker hits from the first grain and are most clearly visible when v_{imp} is rather large. (b) and (c), which are for $v_{\text{imp}} = 10^{-2}$ and 10^{-3} also possess similar features. The tails, however, are more dominant and the additional compressions are no longer so clearly visible.

IV. EFFECTS OF IMPURITIES

We now turn to the question of whether buried light mass impurities can be acoustically detected using backscattering of the solitons sent down the chain. Sand grains are rather

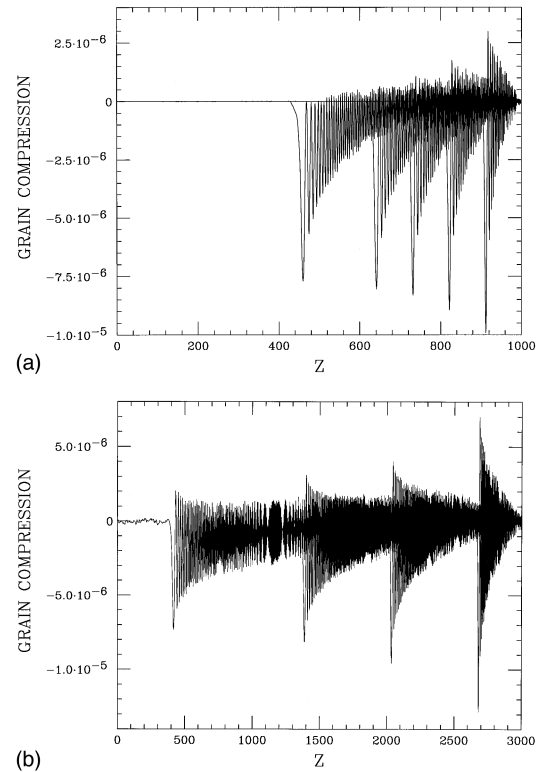


FIG. 3. (a) and (b) Data showing the propagation of pulses with long exponentially decaying tails in depth z (expressed in grain diameters) at various times and for two different combinations of v_{imp} and l_0 values. As in Figs. 1 and 2, the y axis represents the displacement of grains (in program units) from the original equilibrium positions. In (a) $l_0 = 10^{-4}$, $v_{\text{imp}} = 10^{-3}$ and in (b) $l_0 = 10^{-3}$, $v_{\text{imp}} = 10^{-2}$.

heavy objects (density of sand is $\sim 2700 \text{ kg/m}^3$). Thus, most impurities such as rubber, plastic, or wood would be less dense than sand. It is in this spirit that we are especially interested in detecting light impurities. It is instructive to recall here that the dynamical behavior of harmonic oscilla-

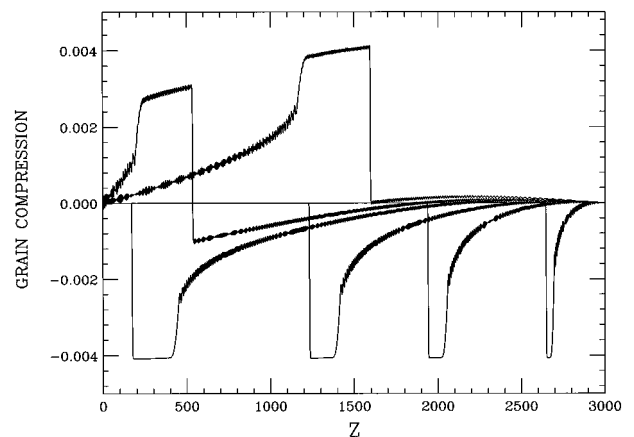


FIG. 4. The figure represents the forward propagation and the reflection of a solitonlike pulse in a regime in which both shocklike and compressive effects are present. The calculations have been done for $v_{\text{imp}} = 10^{-1}$ (i.e., large v_{imp} expressed in program units) and for $l_0 = 10^{-3}$ (i.e., intermediate range loading, also expressed in program units).

tor chains with a single light impurity has been extensively probed by many workers. It is well known that the presence of a light impurity leads to the localization of the perturbation at the light impurity site and that there is a specific frequency that characterizes the localized oscillations of the light impurity [15]. One would expect that long-lived oscillations, albeit over a broad window of frequencies, may persist in light impurities in Hertzian chains as well. As we discuss below, our calculations seem to suggest that such long-lived oscillations may indeed be present in Hertzian chains with light impurities.

Our first studies have been carried out for a horizontal granular chain ($g=0$) of 1000 grains in which the impurity has been placed at the 500th grain. Let us first consider the case of a light impurity with a mass of 0.5. We set the value of $a=2000$. The forward propagating solitonlike pulse and the backscattered signals are shown in Fig. 5(a) for $v_{\text{imp}}=10^{-2}$ and $l_0=10^{-4}$, i.e., in a regime in which significant tails are visible in the solitonlike pulse. The backscattered pulse has an altered tail with respect to that in the in-going pulse, as can be seen in Fig. 5(a). We should point out that the front of the backscattered solitonlike pulse should be most easily detectable at the surface of the chain. However, the front or the “head” of the pulse simply tells one that a reflection has occurred and hence may not be very useful in discriminating between the details of the impurity with significant confidence. The most important information concerning the backscattering process can be obtained from the features in the tail of this pulse. This implies that one must manipulate the parameters l_0 and v_{imp} , as alluded to in Sec. III B above, such that the distinctive features of the tail are most clearly visible.

We now ask the question of whether one gets different backscattered pulses for the light and heavy mass impurities. This is an important issue to be considered if soliton backscattering is to be used to detect buried light mass impurities. We present backscattering data from a heavy and less compressible impurity of mass 2.0 and $a=10\,000$. These data are presented in Fig. 5(b). Although at first sight, the raw data in Figs. 5(a) and 5(b) look rather identical, a careful look reveals that the backscattered pulse from the heavy impurity case possesses a distinctly different tail profile with respect to that for the light impurity case. These differences are illustrated in Fig. 5(c).

Can these differences be experimentally detected? Recently, using microelectromechanical sensors, it has become possible to use capacitive measurements to detect very small scale disturbances in various systems [16]. Therefore, it may well be possible to detect the light mass impurities and separate them from the heavy mass impurities by distinguishing between the detailed features of the tails of backscattered pulses using acoustic backscattering of solitons.

V. EFFECTS OF GRAVITATIONAL COMPACTION AND IMPURITIES

Gravitational compaction is an important aspect of vertical granular columns. In a finite column, the grain at the bottom suffers maximum overlap under such compaction, while the one at the surface is uncompressed. This condition is realized via Eq. (4). The increasing overlap with depth

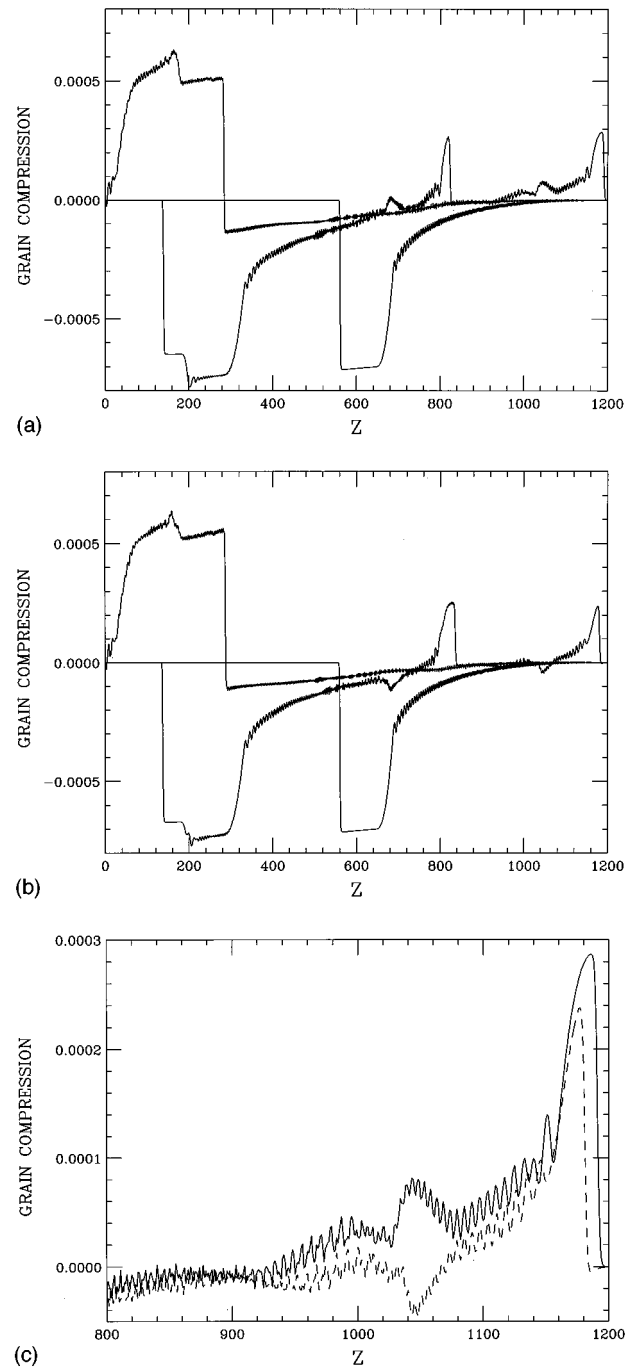


FIG. 5. (a) Plot of grain displacements (in program units) as a function of depth (in grain diameters) for in-going and reflected pulses. The reflection occurs from five light mass impurities which are located symmetrically about the midpoint of the chain. Observe the nonexponential profile of the tail of the pulse. (b) Plot of grain displacements as a function of depth for in-going and reflected pulses when five heavy impurities are placed symmetrically about the midpoint of the chain. The reflected pulse has a very different structure compared to that in (a). The key differences arise from excessive compressions created by the motion of the heavier masses. (c) The dashed and the solid lines illustrate the differences between the grain locations with respect to their original equilibrium positions for the light and the heavy impurity cases, respectively.

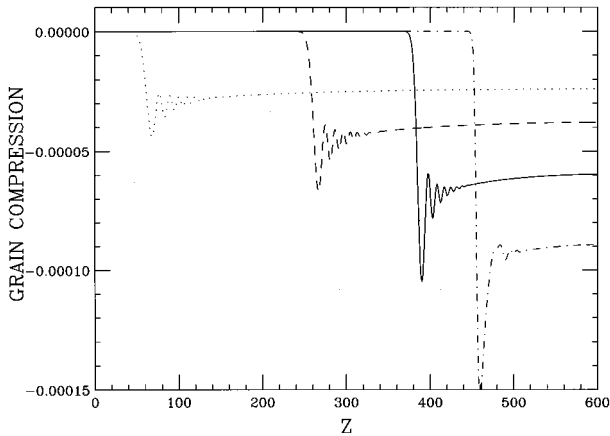


FIG. 6. The data show the granular displacements (in program units) from the original equilibrium positions (in program units) as a function of depth for $g=0.001$ (dotted), $g=0.1$ (long dashes), $g=1.0$ (solid), and $g=10.0$ (dot dashes) in a 600 grain column. $g=1.0$ corresponds to an acceleration of 9.8 m/s^2 . The number of peaks in the pulse increases and the magnitude of the grain displacements decreases as g is increased. The data are all taken after the same amount of time has elapsed since the initiation of the perturbation. Thus, the pulse speed is sensitive to g .

results in an increase in the speed of an acoustic perturbation in the vertical gravitationally compacted grain columns. Particle dynamics simulations of the behavior of sound speed in such columns were reported earlier in Refs. [5] and [6]. For Hertzian contacts, the speed of the fastest moving grain at depth z in a pulse increases as $z^{1/6}$, where z is set to zero at the surface, as shown in the work mentioned above. We focus on the properties of the solitonlike pulse below.

The basic features associated with the solitonlike pulse at nonuniform loading for $v_{\text{imp}}=10^{-1}$ lie in the fact that the square-wave aspect of the pulse is now altered and replaced by a bump with a tail consisting of bumps of decreasing amplitude. These features are illustrated in the calculations presented in Fig. 6, in which the grain positions are presented for three different magnitudes of the gravitational acceleration g . The smaller bumps following the head of the pulse are created by the oscillations that persist as a result of gravitational compaction. It is evident from the data in Fig. 6 that the number of smaller bumps is less and the granular displacements off the original equilibrium positions are larger when the gravitational effects are small. The data for the various values of g were recorded after the same amount of time had elapsed since the initiation of the perturbation. The calculations shown in Fig. 6 suggest that the oscillations of the grains in gravitationally compacted grain columns may help the problem of detecting buried impurities. As discussed in earlier publications [5,6], these data reflect the fact that while sound speed increases with depth z as $z^{1/6}$, the magnitude is sensitive to g , as expected (see Fig. 6) [4–6].

Here we extend the earlier analysis to report on the behavior of the solitonlike pulse when it encounters a small chain of light mass impurities and a corresponding study with heavy mass impurities that are placed in the central region of vertical grain columns at $g=1$. We present our calculations for the velocity of the grains as a function of depth in the column (rather than displaced positions of the

grains as a function of depth) for the light mass parameters considered in Sec. IV. The results are presented in Figs. 7 and 8.

Figures 7(a)–7(f) present the backscattering data for the solitonlike pulse for five adjacent light mass impurities ($m=0.5$, $a=2000$) which are centered about the position of the 500th grain, while Figs. 8(a)–8(f) present the same calculation for a set of five adjacent heavy mass ($m=2.0$ and $a=10\,000$) impurities which are also centered around the 500th grain.

Figures 7(a)–7(d) and 8(a)–8(d) illustrate the grain velocities as a function of position, at various corresponding times, for the chains with five light and five heavy impurities, respectively. Comparison between Figs. 7(d) and 8(d), which present snapshots of the two systems immediately after the incoming perturbation collides with the five impurity chains, reveals that the details of the grain velocities as a function of position are slightly different in the two cases. The differences between the two cases become more apparent as a function of time. Figures 7(e) and 8(e) show differences between (i) the directions of motion of the grains that lie in the leading part of the backscattered pulses, and (ii) the amplitudes of the backscattered signals, the amplitudes being slightly larger for the chain with light impurities. Comparison between Figs. 7(e) and 8(e) and Figs. 7(f) and 8(f) illustrates the robustness of the features in the backscattered pulses in these two idealized chains. We have carried out these calculations with a single light impurity and a single heavy impurity in Hertzian chains. All of the features shown here were also observed in those studies.

Our studies suggest that the leading part of the backscattered pulse consists of compressive motion along the column when the backscattering is from light impurities. For massive impurities, the leading part of the pulse consists of motion that is opposite in direction to that of the original perturbation. These features are significant and robust and, hence, should be detectable in actual experiments.

VI. DRIVEN COLUMNS

We have also carried out studies in long columns of 10 000 grains in which the last grain is held fixed and in which we arranged for the surface grain to oscillate at an amplitude $A=2.0$ (recall $2R=100$) and with a small period $\tau=10$. The oscillatory signal travels down the column and leads to the formation of bands in the column consisting of regions in which the grains are significantly compressed (high grain velocities and kinetic energies) with respect to their nearest neighbors along the direction of propagation of the pulse and inter-band regions in which they are weakly compressed (low grain velocities and kinetic energies) in the direction that is opposite to that of pulse propagation. We present snapshots of the kinetic energy of the grains as a function of depth at various times in Figs. 9(a)–9(f) and of velocity of grains as a function of depth in Figs. 10(a)–10(f). These features are visible in Figs. 9(a) and 10(a). In time, the regions with strong and weak compression effects tend to acquire approximately equal compressions and hence become more symmetric as in Figs. 9(b) and 10(b). Figures 9(c) and 10(c) exhibit regions of very small scale granular motion between the regions of significant compression,

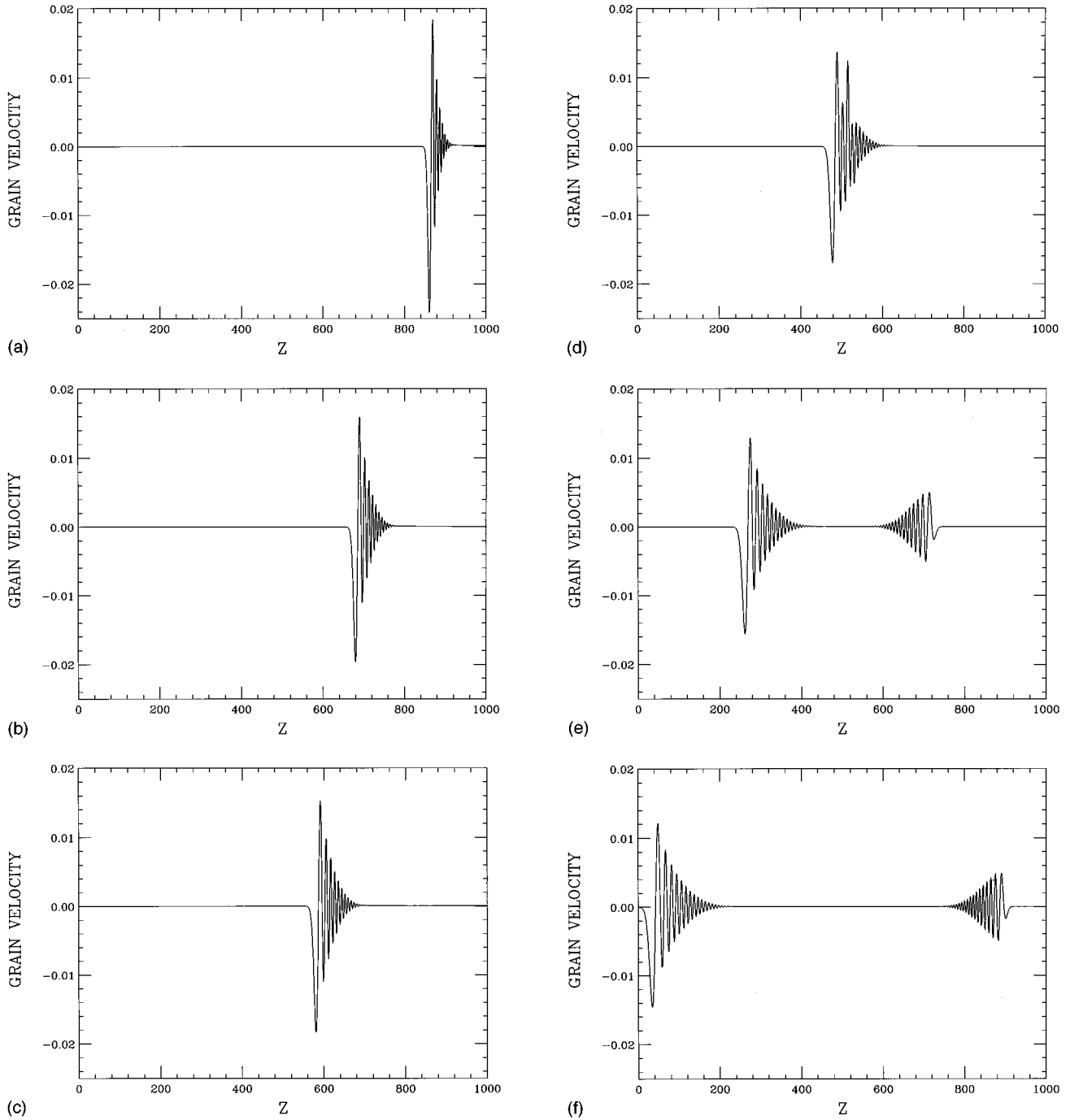


FIG. 7. (a)–(f) Plot of velocity of grains (in program units) as a function of depth as time progresses in a vertical grain column ($g=1$). The light impurities are located symmetrically about position 500. Observe the amplitude and the shape of the reflected pulse.

which tend to give way in Figs. 9(d), 9(e), 10(d), and 10(e) to standing-wave-like patterns, which tend to remain stable over many thousands of integration time steps.

The plots shown have been obtained by averaging over ten time steps which are each 1.25×10^{-4} apart in time. The data suggest that over long times and length scales, there develops standing-wave-like patterns in the column.

VII. DISCUSSION

We have presented particle-dynamics-based simulations on the propagation of perturbations in Hertzian chains. We

have probed the problem of propagation of a solitonlike pulse under various loading conditions described by l_0 and for various initial impacts characterized by v_{imp} in horizontally oriented granular chains, i.e., for $g=0$. For cases in which $l_0 \sim 10^{-6}$, we find that the pulse propagation can be characterized as shocklike. In the shocklike regime, the initial impact dictates the pulse speed, and the dynamical effects associated with the compression and the dilation of the grains which are in contact play a weak role. In this regime, the pulse behaves like a soliton and preserves its identity over space and time as well as during collisions with another solitonic pulse. The latter will be discussed in a separate

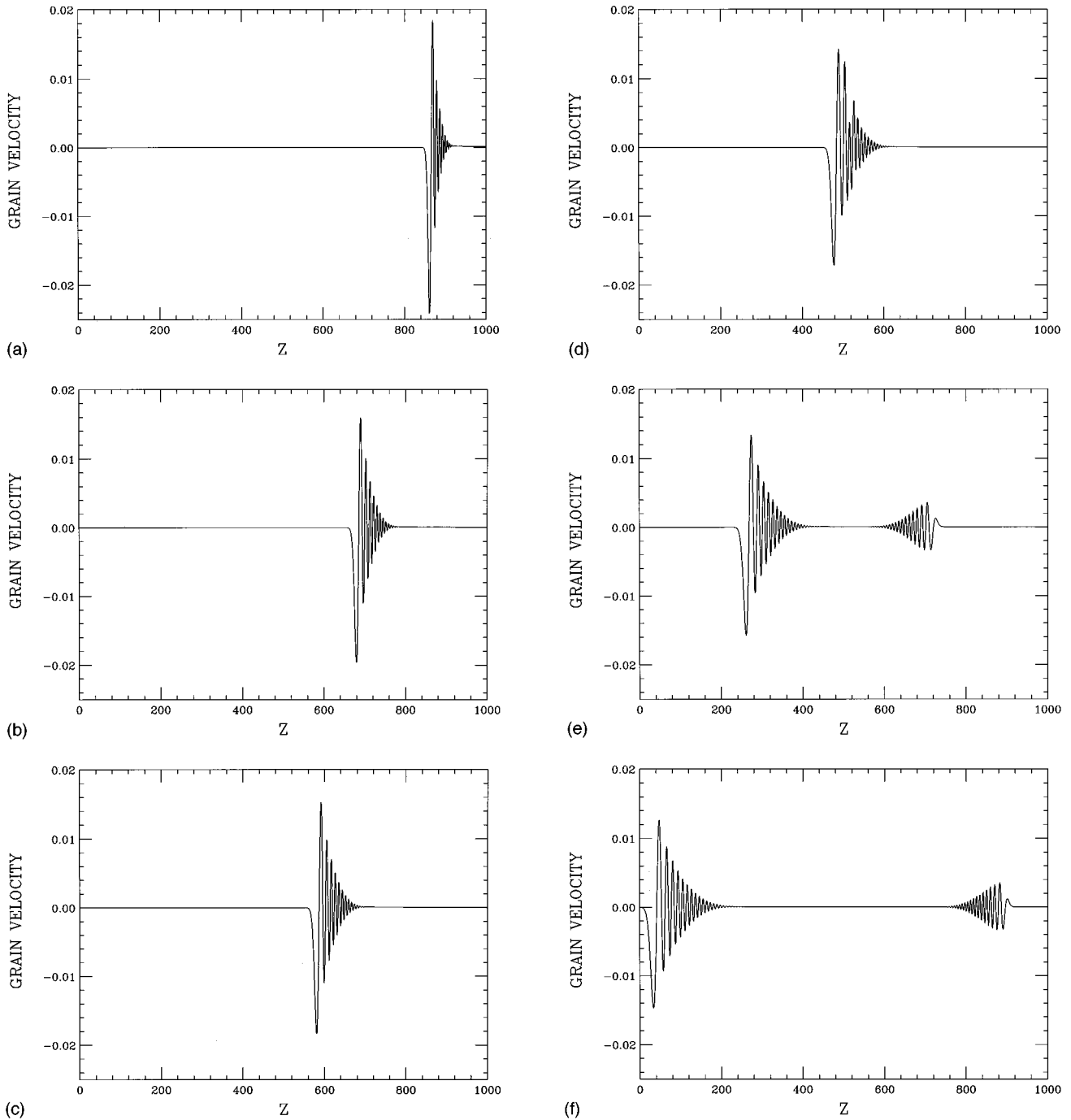


FIG. 8. (a)–(f) The data shown are very similar to those in Figs. 7(a)–7(f) except that now there are five heavy impurities distributed about the 500th grain. The shape of the reflected pulse is different, indicating that the dynamics of the light masses affect the reflected pulse profile.

publication [13]. To our knowledge, Eq. (3) is not widely recognized as a soliton generating equation under appropriate boundary conditions. Preliminary calculations to be discussed elsewhere [13] reveal that the solitonic features persist for potentials in which $V(\delta_{i,i+1}) \sim \delta_{i,i+1}^n$, where $n > 2$.

For larger magnitudes of l_0 , i.e., $l_0 \sim 10^{-3}$ or 10^{-4} , the pulse propagation exhibits effects which are strongly influenced by the dynamical effects associated with the compression of the grains. The pulse shapes when plotted as a function of distances moved by the grains with respect to their

original equilibrium positions versus their positions in the chain, exhibit a head followed by a long exponential tail. Our studies suggest that this tail contains critical details about the system dynamics. We prefer to call the pulse solitonlike in this compressive regime. The pulse suffers slow distortion and contains distinct oscillatory features which are uncharacteristic of perfect solitons.

We have carried out detailed analyses on the problem of backscattering of the solitonlike pulse, under appropriate loading and v_{imp} , from light and heavy mass impurities with $g=0$. In addition, we have probed the problem of soliton

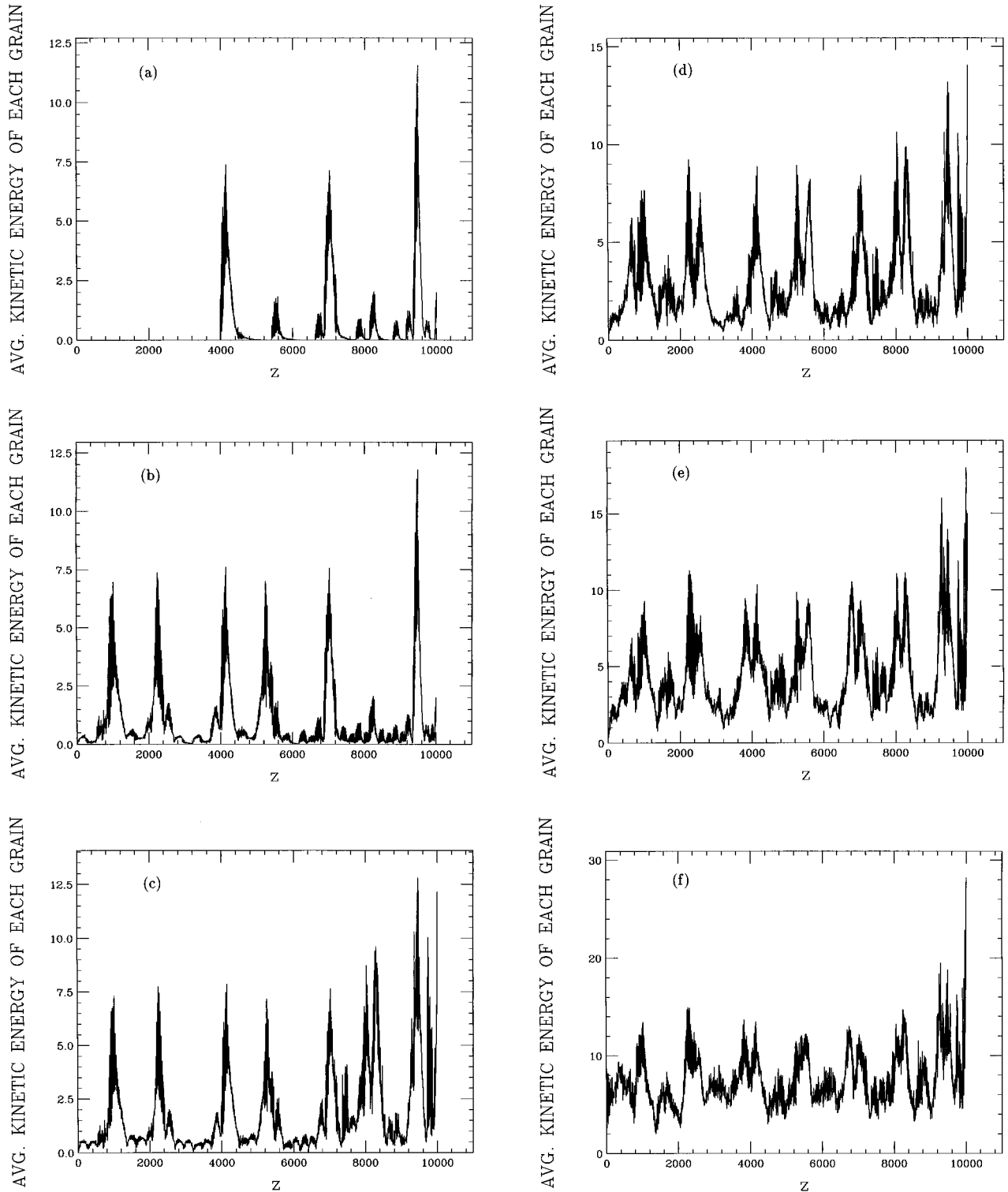


FIG. 9. (a)–(f) Plot of the average kinetic energy of grains (in program units) as a function of their positions (or depths) in the column when the surface grain is being driven by a signal $2\sin 2t\pi/1.012 \times 10^{-3}$ at times $t = 60$ (a), 132 (b), 204 (c), 276 (d), 492 (e), where time is measured in units of 1.012×10^{-3} s. Observe the formation of standing-wave-like patterns at large times. The snapshots have been constructed by averaging the data over 1.5 time units. The integration time step was 1.265×10^{-7} s in these studies.

backscattering for buried light and heavy mass impurities in the presence of gravitational fields. Our studies suggest that the detailed features in the tails of the backscattered pulses are sensitive to the characteristics of the impurity for the $g=0$ problem. The differences between the backscattered pulses are even more dramatic in vertical columns with finite

g . Therefore, these studies promise the possibility of using acoustic signals for detecting certain buried impurities in granular media.

Finally, we have probed the propagation of low frequency sinusoidal signals in long but finite granular columns over three decades in time. Our calculations reveal the formation-

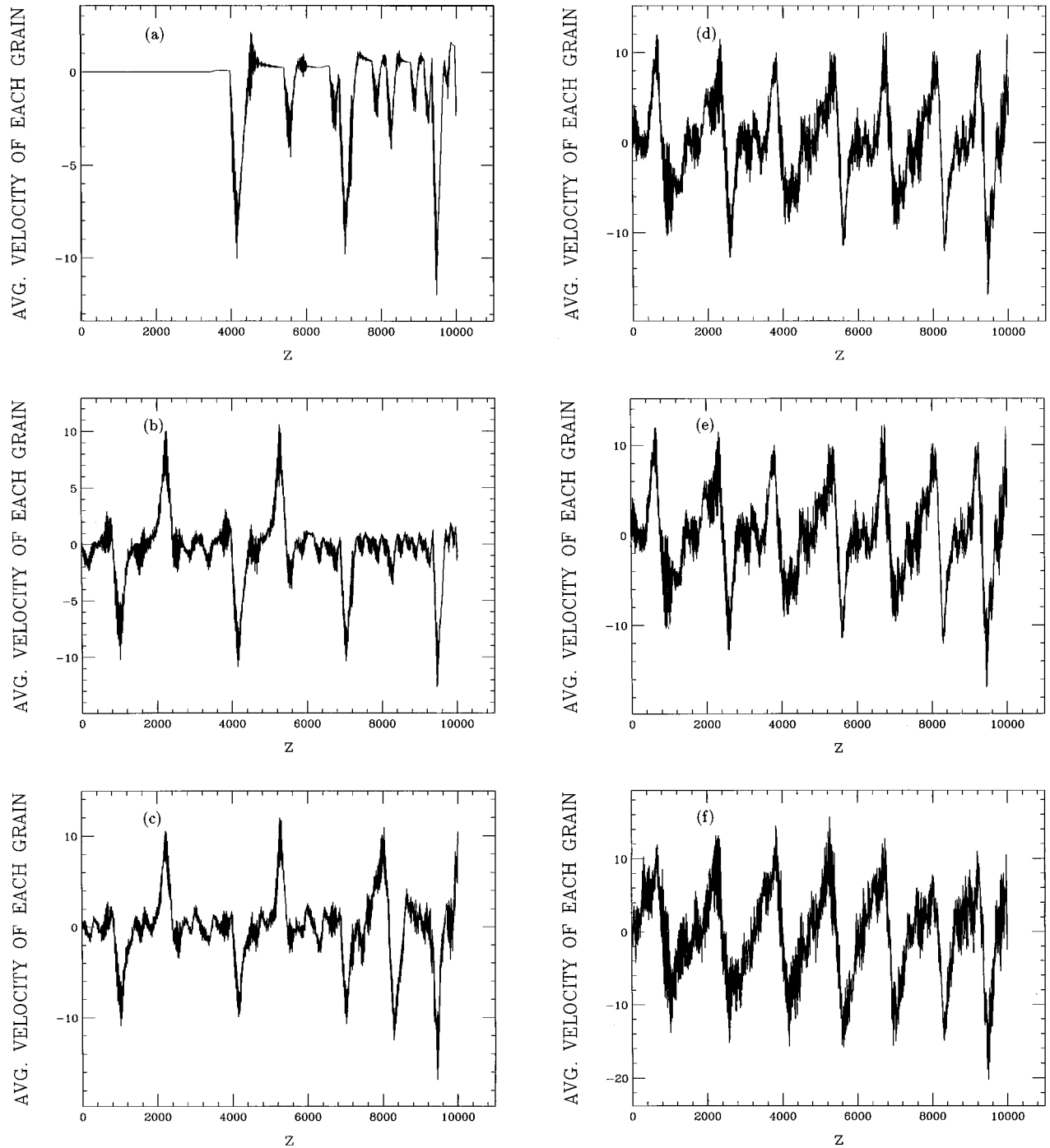


FIG. 10. (a)–(f) Plot of the average velocity of grains as a function of their positions (or depths) in the system in Figs. 9(a)–9(f) at the corresponding times.

of standing-wave-like patterns from the constructive and destructive interference of traveling solitonlike waves. We believe that this is a new result and may have possible interesting applications in measuring positions of buried massive objects in granular beds.

To carry out effective detection of buried impurities in granular beds one must acquire a detailed understanding of the propagation and backscattering of solitonlike pulses that can be generated under appropriate loading conditions and initial impacts. Perhaps the most crucial step in acquiring

this capability lies in one's ability to discriminate between the backscattered pulses from light and heavier impurities.

ACKNOWLEDGMENTS

We are grateful to Robert S. Sinkovits for collaboration in the early phase of this work. S.S. thanks Dr. Alan J. Hurd (Sandia National Laboratories) and Dr. Alexander Britan (Ben Gurion University of the Negev) for their interest in this work. We are also grateful to Dr. Ernie Cespedes of the

U.S. Army Waterways Experiment Station and Professor Michael J. Naughton for many helpful discussions. J.D.W. was partially supported by an exchange agreement between SUNY at Buffalo and the University of Kent at Canterbury,

UK. S.S. and M.M. acknowledge support of the Office of the Provost at SUNY at Buffalo through a Multidisciplinary Project award and the support of the U.S. Army under Contract No. DACA-39-97-K-0026.

-
- [1] P.J. Digby, *J. Appl. Mech.* **48**, 803 (1981).
 [2] V. F. Nesterenko, *Zh. Prik. Mekh. Tekh. Fiz.* **5**, 733 (1983); V. F. Nesterenko, V. M. Pomin, and P. A. Cheskidov, *ibid.* **4**, 130 (1983).
 [3] K. Walton, *J. Mech. Phys. Solids* **35**, 213 (1987).
 [4] J. D. Goddard, *Proc. R. Soc. London, Ser. A* **430**, 105 (1990).
 [5] R. S. Sinkovits and S. Sen, *Phys. Rev. Lett.* **74**, 2686 (1995).
 [6] S. Sen and R. S. Sinkovits, *Phys. Rev. E* **54**, 6857 (1996).
 [7] T. Boutreux, E. Raphaël, and P. G. de Gennes, *Phys. Rev. E* **55**, 5759 (1997).
 [8] C. Coste, E. Falcon, and S. Fauve, *Phys. Rev. E* **56**, 6104 (1997).
 [9] L. D. Miller (private communication).
 [10] See for instance, D. W. McLaughlin, in *Physics in One Dimension*, edited by J. Bernasconi and T. Schneider (Springer, Berlin, 1981).
 [11] A. Britan, T. Elperin, O. Igra, and J. P. Jiang, in *Shock Compression of Condensed Matter, 1995*, AIP Conf. Proc. No. 370, Part 1, edited by S. C. Schmidt and W. C. Tao (AIP, New York, 1995), p. 971; A. Britan, G. Ben-Dor, T. Elperin, O. Igra, and J. P. Jiang, *Exp. Fluids* **22**, 433 (1997).
 [12] L. D. Landau and E. M. Lifshitz, *Theory of Elasticity* (Pergamon, Oxford, 1970), p. 30; H. Hertz, *J. Math.* **92**, 156 (1881).
 [13] M. Manciu and S. Sen (unpublished).
 [14] M. P. Allen and D. J. Tildesley, *Computer Simulation of Liquids* (Clarendon, Oxford, 1987).
 [15] See, for instance, M. H. Lee, J. Florencio, Jr., and J. Hong, *J. Phys. A* **22**, L331 (1989), and references therein; S. Sen, Z.-X. Cai, and S. D. Mahanti, *Phys. Rev. Lett.* **72**, 3287 (1994).
 [16] M. J. Naughton, J. P. Ulmet, A. Narjis, S. Askenazy, M. V. Chaparala, and A. P. Hope, *Rev. Sci. Instrum.* **68**, 4061 (1997).